

Molecular Cancer Therapeutics



Selective Targeting of Interferon γ to Stromal Fibroblasts and Pericytes as a Novel Therapeutic Approach to Inhibit Angiogenesis and Tumor Growth

Ruchi Bansal, Tushar Tomar, Arne Östman, et al.

Mol Cancer Ther 2012;11:2419-2428. Published OnlineFirst August 29, 2012.

Updated version	Access the most recent version of this article at: doi: 10.1158/1535-7163.MCT-11-0758
Supplementary Material	Access the most recent supplemental material at: http://mct.aacrjournals.org/content/suppl/2012/08/29/1535-7163.MCT-11-0758.DC1.html

Cited Articles	This article cites by 38 articles, 8 of which you can access for free at: http://mct.aacrjournals.org/content/11/11/2419.full.html#ref-list-1
Citing articles	This article has been cited by 1 HighWire-hosted articles. Access the articles at: http://mct.aacrjournals.org/content/11/11/2419.full.html#related-urls

E-mail alerts	Sign up to receive free email-alerts related to this article or journal.
Reprints and Subscriptions	To order reprints of this article or to subscribe to the journal, contact the AACR Publications Department at pubs@aacr.org .
Permissions	To request permission to re-use all or part of this article, contact the AACR Publications Department at permissions@aacr.org .

Selective Targeting of Interferon γ to Stromal Fibroblasts and Pericytes as a Novel Therapeutic Approach to Inhibit Angiogenesis and Tumor Growth

Ruchi Bansal¹, Tushar Tomar¹, Arne Östman³, Klaas Poelstra^{1,2}, and Jai Prakash^{1,2,3,4}

Abstract

New approaches to block the function of tumor stromal cells such as cancer-associated fibroblasts and pericytes is an emerging field in cancer therapeutics as these cells play a crucial role in promoting angiogenesis and tumor growth via paracrine signals. Because of immunomodulatory and other antitumor activities, IFN γ , a pleiotropic cytokine, has been used as an anticancer agent in clinical trials. Unfortunately only modest beneficial effects, but severe side effects, were seen. In this study, we delivered IFN γ to stromal fibroblasts and pericytes, considering its direct antifibrotic activity, using our platelet-derived growth factor-beta receptor (PDGFR)-binding carrier (pPB-HSA), as these cells abundantly express PDGFR. We chemically conjugated IFN γ to pPB-HSA using a heterobifunctional PEG linker. *In vitro* in NIH3T3 fibroblasts, pPB-HSA-IFN γ conjugate activated IFN γ -signaling (pSTAT1 α) and inhibited their activation and migration. Furthermore, pPB-HSA-IFN γ inhibited fibroblasts-induced tube formation of H5V endothelial cells. *In vivo* in B16 tumor-bearing mice, pPB-HSA-IFN γ rapidly accumulated in tumor stroma and pericytes and significantly inhibited the tumor growth while untargeted IFN γ and pPB-HSA carrier were ineffective. These antitumor effects of pPB-HSA-IFN γ were attributed to the inhibition of tumor vascularization, as shown with α -SMA and CD-31 staining. Moreover, pPB-HSA-IFN γ induced MHC-II expression specifically in tumors compared with untargeted IFN γ , indicating the specificity of this approach. This study thus shows the impact of drug targeting to tumor stromal cells in cancer therapy as well as provides new opportunities to use cytokines for therapeutic application. *Mol Cancer Ther*; 11(11); 2419–28. ©2012 AACR.

Introduction

In the past decade, the complexity of the tumor micro-environment has been extensively studied, and this knowledge has contributed to the development of new therapies for cancer (1). Apart from cancer cells, solid tumors contain large amounts of tumor stroma comprising a variety of cell types such as cancer-associated fibroblasts (CAF), pericytes, endothelial cells, infiltrated immune cells, and cancer stem cells. Among them, CAFs

are the major cell type that play a crucial role in tumorigenesis and metastasis (1, 2) by secreting various cytokines and growth factors (e.g., VEGF, HGF, SDF-1 α), which act in a paracrine/exocrine fashion on other cell types, thereby activating tumor-inducing processes (2–4). In addition to CAFs, pericytes are another important cell type, having phenotypic characteristics of mesenchymal cells and fibroblasts. These pericytes stabilize endothelium by surrounding the blood vessels and support angiogenesis by secreting VEGF (1). Both stromal fibroblasts and pericytes, collectively referred here as stromal cells, express high levels of platelet-derived growth factor-beta receptor (PDGFR) and its expression in tumor stroma has been inversely correlated with the survival rate in patients with different types of cancer (5, 6). Also, studies have shown that inhibition of the functions of these stromal cells using a PDGFR inhibitor (imatinib) leads to inhibition of angiogenesis and thereby reduction in tumor growth (7, 8). These data indicate the key role of the tumor stromal cells in tumor development; therefore, selective targeting to stromal cells for cancer therapeutics is of great interest and could provide highly attractive strategies to treat cancer.

Among potent anticancer agents, IFN γ has been shown to possess multiple potent antitumor properties. IFN γ is a

Authors' Affiliations: ¹Department of Pharmacokinetics, Toxicology and Targeting, Graduate School for Drug Exploration (GUIDE), University of Groningen; ²BiOrion Technologies BV, MediTech Centre UMCG, L.J. Zielstraweg 1, Groningen, The Netherlands; ³Cancer Centre Karolinska, Department of Oncology-Pathology, Karolinska Institutet, Stockholm, Sweden; and ⁴Department of Targeted Therapeutics, MIRA Institute of Biomedical Technology and Technical Medicine, University of Twente, Enschede, The Netherlands

Note: Supplementary data for this article are available at Molecular Cancer Therapeutics Online (<http://mct.aacrjournals.org/>).

Corresponding Author: Jai Prakash, Department of Targeted Therapeutics, MIRA Institute of Biomedical Technology and Technical Medicine, University of Twente, Enschede, The Netherlands. Phone: 31-53-489-2412; Email: j.prakash@utwente.nl

doi: 10.1158/1535-7163.MCT-11-0758

©2012 American Association for Cancer Research.

immunomodulatory cytokine produced by immune cells (mainly natural killer cells and subsets of T cells) and is physiologically involved in promoting innate and adaptive immune responses (9). It interacts with the IFN γ receptor and activates the JAK-STAT1 signaling pathway, which regulates transcription of various genes. IFN γ , apart from its physiologic functions, has been extensively explored as a therapeutic cytokine for various diseases such as immunodeficiency diseases, chronic inflammatory diseases, fibrosis, tumors, and atypical mycobacterial infections in pre-clinical studies (10–12). However, most clinical trials failed (13–16) and its clinical application is limited because of its side effects on nontarget cells as IFN γ receptors are present on almost all cell types. The antitumor response of IFN γ has been shown to be mainly associated with its immunologic effects, but also nonimmunologic effects such as direct killing of tumor cells and inhibition of proliferation of endothelial cells have been proposed. In addition, IFN γ has been shown to display strong antifibrotic effects in different fibrosis models in lung, liver, and kidneys (17–20) by inhibiting activation and proliferation of fibroblasts.

As stromal cells highly contribute to angiogenesis and tumor growth, we hypothesized that interference in the tumor-promoting activities of these cells by the local delivery of IFN γ might inhibit the tumor growth. We have designed a PDGF β R-recognizing drug carrier (pPB-HSA) composed of PDGF β R-binding cyclic peptides (pPB) conjugated to human serum albumin (HSA; ref. 21, 22) for specific targeting to PDGF β R-expressing tumor stromal cells. Furthermore, we have shown that pPB-mediated targeting of IFN γ to hepatic stellate cells, expressing high levels of PDGF β R during liver fibrosis, completely abolished advanced liver cirrhosis in mice (23). In this study, we delivered IFN γ to stromal fibroblasts and pericytes using pPB-HSA carrier to impair angiogenesis thereby inhibiting the tumor growth, whereas avoiding IFN γ -mediated off-target effects. To effectuate this, we conjugated IFN γ to pPB-HSA and examined the synthesized conjugate for its therapeutic efficacy *in vitro* and *in vivo*.

Materials and Methods

Cell lines

Murine NIH3T3 fibroblasts, B16-F10 melanoma cells, and RAW264.7 macrophages were obtained from American Type Culture Collection. H5V heart capillary endothelial cell line was kindly provided by Dr. A. Vecchi (Mario Negri, Institute for Pharmacological Research, Milan, Italy) to UMCG Groningen. RAW264.7, NIH3T3, H5V, and B16 cells were cultured in Dulbecco's Modified Eagle's Medium (Invitrogen) supplemented with 10% fetal bovine serum (FBS) and antibiotics. No authentication for cell lines was done by the authors.

Synthesis and characterization of pPB-HSA-IFN γ conjugate

The synthesis procedure of pPB-HSA-IFN γ conjugate has been described earlier (24). The brief methodology has

been provided in the supplementary methods. The pPB-HSA-IFN γ conjugate was characterized using Western blot analyses and the biologic activity was assessed with a nitric oxide release assay in RAW cells as described earlier (24).

In vitro binding of the IFN γ conjugate to mouse 3T3 fibroblasts

Cells were cultured overnight in Lab-Tek (Nunc) and incubated with pPB-HSA-IFN γ (1 μ g/mL) for 2 hours. To block the PDGF β R-mediated binding, anti-PDGF β R immunoglobulin G (IgG; Santa Cruz Biotechnology) was added 1 hour before adding IFN γ conjugate. Then, cells were stained with anti-pPB antibody.

In vitro effects of the IFN γ conjugate in mouse 3T3 fibroblasts

Cells (3×10^4 cells/24-well and 7.5×10^4 cells/12-well plate) were cultured for overnight and starved with 0.5% FBS containing medium for 24 hours. Cells were then incubated with 5 ng/mL human recombinant TGF β 1 (Roche) with or without IFN γ (16 nmol/L), pPB-HSA-IFN γ (equivalent to 16 nmol/L IFN γ), and pPB-HSA (molar equivalent) for 48 hours. Subsequently, cells were stained for collagen-I or α -SMA and were analyzed for gene expression (Supplementary Materials and Methods).

The IFN γ signaling p-STAT1 α was analyzed using Western blot analysis in 3T3 fibroblasts, 24 hours after incubating with different compounds as mentioned above. Western blot analysis was carried out from the cell lysates using rabbit monoclonal anti-pSTAT1 α antibody (1:1000, Cell signaling technology Inc.) and β -actin (1:5000, Sigma) as detailed in Supplementary Materials and Methods.

Wound-healing assay

NIH3T3 cells were grown for 24 hours and starved overnight in 0.5% FBS containing medium. A standardized scratch was made using a 200 μ L pipette tip fixed in a holder. Then, cells were incubated with IFN γ (16 nmol/L), pPB-HSA-IFN γ (equivalent to 16 nmol/L IFN γ), or pPB-HSA (molar equivalent). Digital pictures of wounds were captured at $t = 0$ hour and $t = 24$ hours and were analyzed by NIH-ImageJ software to calculate the area of the scratch wound and represented as the percentage of wound healed relative to the controls.

To study the indirect effect of fibroblasts (3T3) on tumor cells (B16), 3T3 cells (1×10^5) were grown for 24 hours, starved for overnight, and then incubated with TGF β (5 ng/mL) with or without IFN γ (16 nmol/L), pPB-HSA-IFN γ (equivalent to 16 nmol/L IFN γ), or pPB-HSA for 24 hours. Thereafter, cells were washed thrice and incubated with fresh starved medium for 24 hours. This conditioned medium was put on B16 cells (5×10^4 , cultured for 48 hours) to carry out the wound-healing assay as described above.

In vitro matrigel tube-formation assay

The fibroblast-mediated paracrine effects of IFN γ and pPB-HSA-IFN γ conjugate on endothelial cells (H5V) were examined using the matrigel tube-formation assay (25). In brief, 3T3-conditioned medium collected after different treatments as mentioned above was added to H5V cells (4×10^4) plated on the matrigel-coated 8-chamber slides (Lab-Tek). VEGF (10 ng/mL, Peprotech) was used as a positive control and added directly to H5V cells. After 20 hours incubation, tubes were visualized, counted, and represented as relative percentage of tube formation.

Subcutaneous B16 tumor mouse model

All animals (male C57BL/6 mice, 20–22 g, Harlan) received *ad libitum* normal diet and 12-hour light–dark cycle. Experimental protocols were approved by the Animal Ethics Committee (University of Groningen). Subcutaneous tumors were induced by injecting B16 cells (1×10^6 cells/100 μ L PBS/mouse) in the left flank. Tumor size was measured using a digital vernier caliper and tumor volume was established using the following formula ($a \times b^2/2$), where a and b denote the length and width of a tumor, respectively.

To determine the therapeutic efficacy, on day 5 after tumor cell injection (when tumors were formed) mice were randomized into 4 groups and were injected intravenously with 5 μ g IFN γ /mouse/day ($n = 5$), pPB-HSA-IFN γ (equivalent to 5 μ g IFN γ , $n = 5$), pPB-HSA (molar equivalent to pPB-HSA-IFN γ , $n = 4$), or vehicle (PBS, $n = 5$) on days 5, 7, 9, 11, 13, 15, and 17. IFN γ amount in the conjugate was analyzed by Western blot analysis. The IFN γ dose was based on our previous studies in liver fibrosis and literature (26, 27). Animals were sacrificed and blood, tumors, and other organs were collected for further analysis. To examine the IFN γ R signaling (pSTAT1 α) *in vivo*, 20 μ g of protein from tumor lysates were analyzed by Western blot analysis using anti-pSTAT1 α , STAT1 α , and β -actin antibodies.

For the biodistribution of pPB-HSA-IFN γ in B16 tumor-bearing mice with tumor size of approximately 2,000 mm³, a single dose (5 μ g/mouse) of pPB-HSA-IFN γ was injected intravenously 15 minutes before sacrifice. Cryosections from tumors and other tissues were stained with anti-pPB IgG for *in vivo* localization.

Immunohistochemistry and immunofluorescence

Cryosections (4 μ m) of tumors and organs were cut and the staining protocol was followed as described earlier (23). Antibodies with their dilution and the detailed method have been described in Supplementary Methods.

Statistical analyses

Data are presented as the mean \pm SEM. Multiple comparisons between different groups were carried out by 1-way ANOVA with Bonferroni posttest unless otherwise mentioned in the figure legends.

Results

Expression of IFN γ R-II and PDGF β R receptors in subcutaneous B16 tumors and other tissues in mice

We initially compared IFN γ R-II and PDGF β R expression in B16 tumors and other organs and found that both receptors were highly expressed in tumor stroma (Supplementary Fig. S1). In other organs, IFN γ R-II was also strongly expressed but PDGF β R expression was low as compared with tumors. In addition, many immune cells especially macrophages strongly express IFN γ R-II (28). Systemic administration of IFN γ will therefore elicit effects in multiple cells in many different organs and immune cells, and distribution to tumors will be relatively low. The high PDGF β R expression on tumor stromal cells in tumors relative to all other tissues supports our notion for the suitability of this receptor for cell-selective targeting of IFN γ .

Characterization of pPB-HSA-IFN γ conjugate

Western Blot analysis of the synthesized PDGF β R-targeted IFN γ conjugate (see diagram in Fig. 1A) using anti-HSA and anti-IFN γ antibodies showed coupling of about 2 IFN γ per pPB-HSA molecule. Nitric oxide release assay in murine RAW264.7 monocytes showed that there was no loss of biologic activity of pPB-HSA-IFN γ as also shown earlier (24). A clear binding of pPB-HSA-IFN γ to 3T3 cells was observed, which was strongly inhibited by anti-PDGF β R IgG, showed its PDGF β R-related specificity (Fig. 1B). Upregulation of PDGF β R expression on 3T3 fibroblasts after activation with TGF β (Fig. 1C) favors the binding of the construct to the activated fibroblasts and pericytes, known to express high PDGF β R (2, 4).

Modification of IFN γ might cause a loss of activity, however activation of pSTAT1 α signaling and MHC-II expression in 3T3 cells by pPB-HSA-IFN γ clearly indicate a full retention of the IFN γ -related activity after chemical modification (Fig. 1D).

pPB-HSA-IFN γ inhibits fibroblasts activation

Furthermore, we investigated the inhibitory effects of IFN γ conjugate on fibroblast activation. Both IFN γ and pPB-HSA-IFN γ substantially inhibited TGF β -induced activation of 3T3 fibroblasts as shown by protein and gene expression of α -SMA (Fig. 2A and B). In addition, they inhibited TGF β -induced protein and gene expression of collagen-I and fibronectin-I ($P < 0.01$; Supplementary Fig. S2A–S2C). In contrast, no inhibitory effects of pPB-HSA rules out the possibility of PDGF β R-blocking effects. Furthermore, IFN γ or pPB-HSA-IFN γ significantly inhibited the migration of fibroblasts, as shown with wound-healing assay (Fig. 2D). Earlier, we have shown that targeted IFN γ inhibits the PDGF-BB-induced proliferation of fibroblasts (24). In our wound-healing assay, however, absence of apoptosis and TGF β -related proliferation stresses that inhibition of wound healing was mainly caused by inhibition of cell migration (Supplementary Fig. S2C and S2D). These results show that both IFN γ

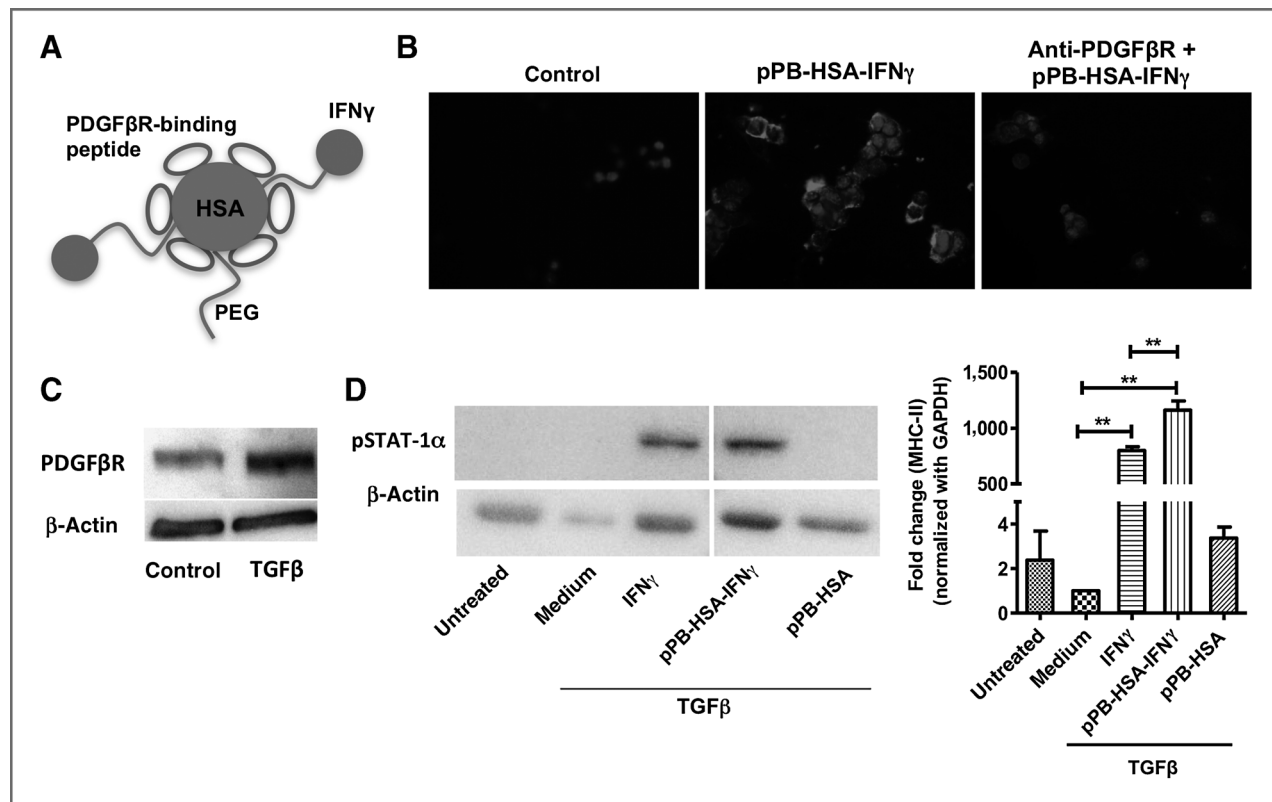


Figure 1. Structure and *in vitro* characterization of pPB-HSA-IFN γ conjugate. **A**, a diagrammatic structure of pPB-HSA-IFN γ conjugate. **B**, fluorescent photographs showing binding of pPB-HSA-IFN γ to mouse 3T3 fibroblasts using anti-pPB immunostaining, which was blocked by anti-PDGFR β antibody. **C**, representative bands from the Western blotting showing increased PDGFR β expression in TGF β -activated 3T3 fibroblasts. **D**, Western blot analyses of pSTAT-1 α and qPCR analysis of MHC-II in 3T3 cells after the treatment with TGF β (5 ng/mL) with or without IFN γ (16 nmol/L), pPB-HSA-IFN γ (equivalent to 16 nmol/L IFN γ), or pPB-HSA alone. All samples were blotted at the same time and blots were analyzed with the same exposure time. GAPDH, glyceraldehyde-3-phosphate dehydrogenase; mean \pm SEM; $n = 3$; **, $P < 0.01$.

and PDGFR β -targeted IFN γ can block the activation and migration of fibroblasts.

pPB-HSA-IFN γ inhibits fibroblast-mediated activation of endothelial cells

Tumor-associated stromal fibroblasts and pericytes activate endothelial cells in a paracrine manner by secreting cytokines and thereby induce angiogenesis (1). In our fibroblasts-induced angiogenesis *in vitro* model, we found that the conditioned media derived from TGF β -stimulated fibroblasts but after removal of stimuli enhanced tube formation compared with that of unstimulated media (Fig. 3A and B), which was similar to that achieved with VEGF, an endogenous angiogenesis-inducing growth factor. Interestingly, conditioned media derived from 3T3 cells treated with IFN γ or pPB-HSA-IFN γ significantly diminished the TGF β -induced tube formation capability of fibroblasts ($P < 0.01$; Fig. 3). Of note as the conditioned media lacked all the added stimuli, no direct effect of IFN γ or its construct on endothelial cells was exhibited. As TGF β did not cause any proliferative effect on fibroblasts and also the treatments did not cause any changes in proliferation and apoptosis of fibroblasts

(Supplementary Fig. S2), the paracrine effects of 3T3 cells were only dependent on the change in the activation state of the cells. These data indicate that selective inhibition of fibroblasts activation with our targeted IFN γ construct may inhibit endothelial cells activation and thereby angiogenesis.

pPB-HSA-IFN γ specifically accumulates in stromal fibroblasts and pericytes *in vivo*

To show the tumor stroma targeting *in vivo*, we investigated the accumulation of pPB-HSA-IFN γ in tumors and various organs, 15 minutes after intravenous injections. Using anti-pPB immunostaining, we found that pPB-HSA-IFN γ rapidly accumulated in tumors especially in tumor stroma (Fig. 4A) where PDGFR β was highly expressed (see Supplementary Fig. S1). pPB-HSA-IFN γ was also found in livers where pPB staining was localized in the sinusoidal lumina. In other organs such as kidneys, heart, and lungs, there was almost no staining detectable (Fig. 4A), which correlates with the low PDGFR β expression in these organs (see Supplementary Fig. S1). As pericytes surrounding tumor endothelium express high PDGFR β , we carried

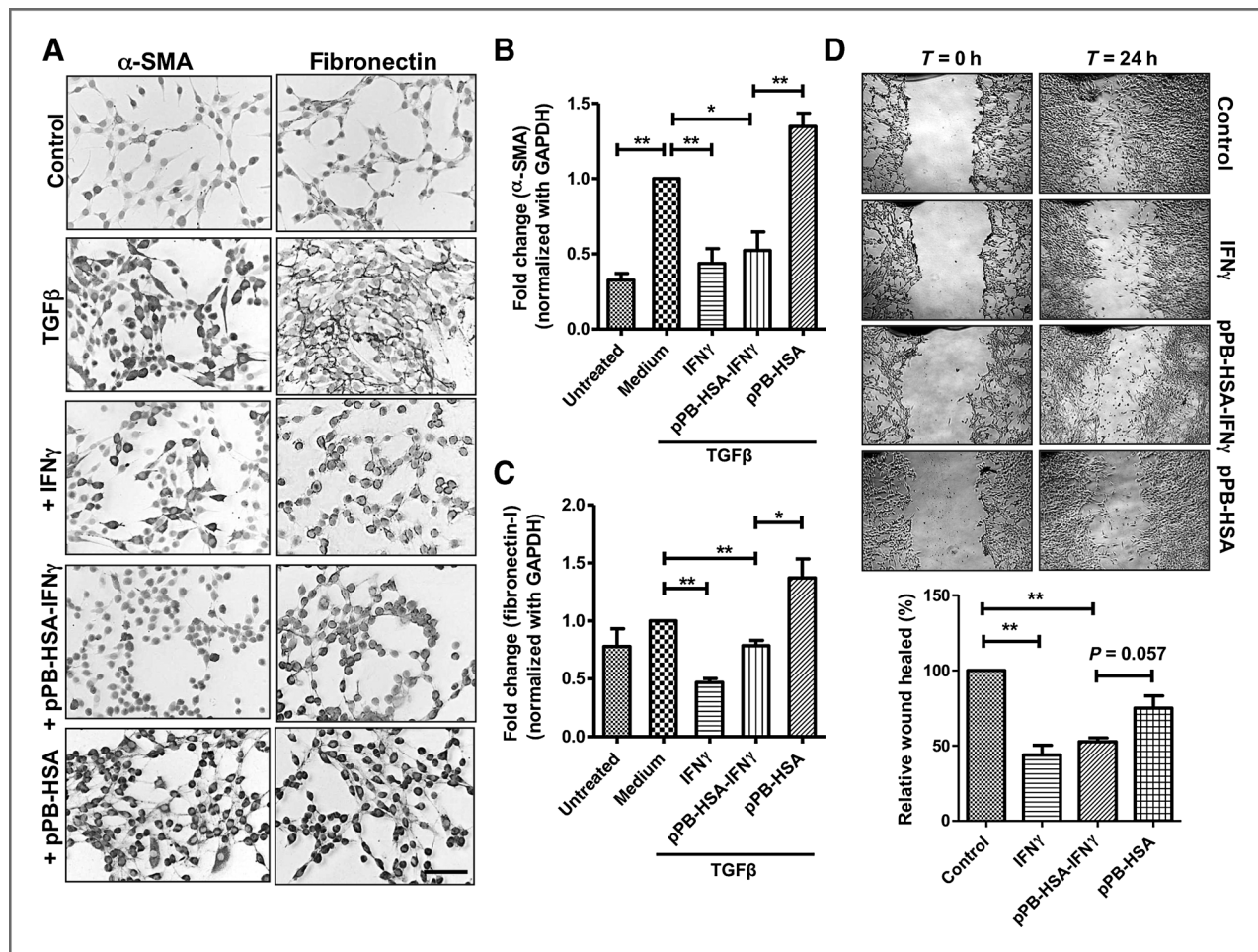


Figure 2. *In vitro* inhibitory effects of pPB-HSA-IFN γ in mouse 3T3 fibroblasts. A, representative microphotographs showing α -SMA and fibronectin-I staining in 3T3 fibroblasts, incubated with TGF β (5 ng/mL) with or without IFN γ (16 nmol/L), pPB-HSA-IFN γ (equivalent to 16 nmol/L IFN γ), or pPB-HSA alone. Scale bars, 100 μ m. QPCR analysis of α -SMA (B) and fibronectin-I (C) in 3T3 fibroblasts. D, representative microscopic images and analysis of wound-healing assay in 3T3 fibroblasts 24 hours after the incubation with IFN γ (16 nmol/L), pPB-HSA-IFN γ (equivalent to 16 nmol/L IFN γ), or pPB-HSA (equivalent). GAPDH, glyceraldehyde-3-phosphate dehydrogenase; mean \pm SEM; $n = 3$; *, $P < 0.05$; **, $P < 0.01$.

out coimmunostaining for PDGF β R and pPB-HSA-IFN γ (anti-pPB), and found a colocalization of the conjugate with pericytes (Fig. 4B). These results show that pPB-HSA-IFN γ conjugate specifically accumulates into PDGF β R-expressing tumor stromal fibroblasts and pericytes.

pPB-HSA-IFN γ reduces tumor growth *in vivo* by inhibition of angiogenesis

In B16-F10 subcutaneous tumor-bearing mice, treatment with pPB-HSA-IFN γ significantly reduced the progression of this malignant tumor (Fig. 4C) whereas PBS, IFN γ , or pPB-HSA did not inhibit it. The enhanced antitumor effect of the targeted construct was attributed to an increased tumor uptake of pPB-HSA-IFN γ as also shown by the activation of the IFN γ signaling (pSTAT1 α) in tumors from pPB-HSA-IFN γ -treated animals ($P < 0.05$ vs. PBS) as compared with other treatment groups (Fig. 5A).

We further explored the effect of the targeted construct on stromal cells and found that α -SMA-positive cells (fibroblasts and pericytes) were markedly less prevalent in targeted IFN γ -treated tumors compared with control tumors (Fig. 5B). Also, there was a significant reduction ($P < 0.01$) in the pericyte population in pPB-HSA-IFN γ -treated mice, as shown with reduction of α -SMA staining around the blood vessels (Fig. 5B). In line with our *in vitro* tube formation assays, we found a significant reduction ($P < 0.01$ vs. IFN γ or pPB-HSA) in angiogenesis with the construct, as shown with the quantitative analysis of CD31-stained lumen area of tumor blood vessels (Fig. 5C). In addition, we carried out cleaved caspase-3 staining in tumors and found that neither free IFN γ nor pPB-HSA-IFN γ -induced apoptosis (data not shown), excluding a possibility of direct proapoptotic effect of the compounds on tumors. As IFN γ is a proinflammatory cytokine and tumor inhibitory effects of the conjugate could be immune-mediated, we carried out CD68 (a common

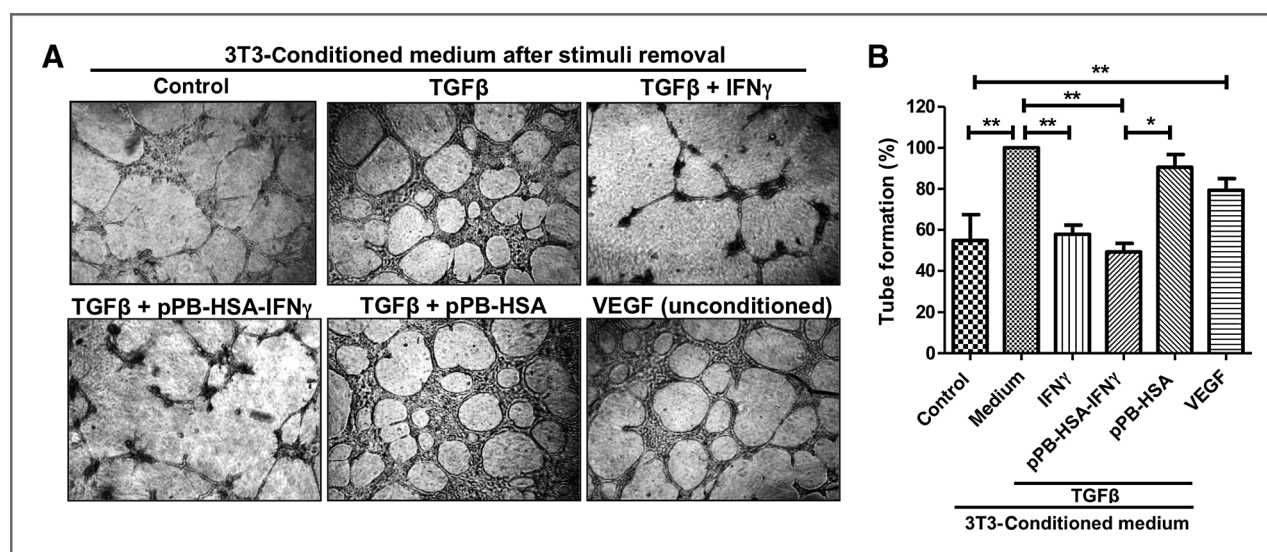


Figure 3. *In vitro* inhibition of paracrine effect of activated fibroblasts on endothelial cells. A, representative pictures of endothelial cell tube formation after incubation with conditioned medium from 3T3 cells that were treated with medium alone (control), TGF β (5 ng/mL) with or without IFN γ (16 nmol/L), pPB-HSA-IFN γ (equivalent to 16 nmol/L IFN γ), or pPB-HSA. Magnification, $\times 40$. B, tubes were counted 24 hours following incubations. VEGF (10 ng/mL) was used directly on H5V cells as a positive control. Mean \pm SEM; $n = 3$; *, $P < 0.05$; **, $P < 0.01$.

marker for monocytes, macrophages, kupffer cells, dendritic cells), CD4, and CD8 (markers for T-lymphocytes) stainings on the tumor tissues and found no significant differences among different treatment groups (Supplementary Fig. S3). These data show that the most of beneficial effects of targeted IFN γ are attributed to the direct inhibition of stromal fibroblasts- and pericyte-supported blood vessel formation.

To examine the effect of targeted IFN γ on other organs, we carried out MHC-II immunostaining in tumors and liver, lungs, and kidneys and carried out semiquantitative analyses. We found that targeted IFN γ -induced MHC-II expression significantly more in tumors compared with other treatments (Fig. 6). In other organs, there was no significant increase with any of the treatments. In the biodistribution study, we observed the distribution of the conjugate in liver sinusoids, but absence of liver inflammation (detected by CD68 immunostaining; Supplementary Fig. S3) in the conjugate-treated livers rules out the possibility of side effects in liver. Furthermore, we examined the body weight and blood parameters in all groups and found no adverse effects of the treatments (Supplementary Table S1 and Supplementary Fig. S4).

Taken together, these results show that selective targeting of IFN γ to tumor stroma inhibits tumor growth indirectly by inhibition of angiogenesis. The targeted construct displayed significantly more potent antitumor activity than native IFN γ , with no significant side effects in other organs.

Discussion

The present study reveals that specific targeting of IFN γ to stromal fibroblasts and pericytes through a PDGF β receptor-recognizing carrier leads to inactivation of these

key cell types in tumors and thereby reduces the tumor growth *in vivo*. Epithelial-derived tumors are generally characterized by the generation of mesenchymal-derived stromal cells, including intratumoral and peritumoral fibroblasts and tumor vasculature-associated pericytes. The paracrine signals induced by these cells have been implicated in tumor growth, angiogenesis, invasion, and metastasis (2, 3). Selective targeting of antifibrotic compounds to these cells, as shown with IFN γ in the present study, may therefore pose a novel approach for the development of a new potential anticancer therapy.

Cell-specific targeting to stromal cells is an unexplored area of research and so far only small molecule inhibitors of Hedgehog, fibroblasts activation protein and PDGFR have been used to show the anti-stromal effects on tumor growth (8, 29, 30) and drug uptake (7, 31). Until now, IFN γ has been shown to possess no/moderate anticancer activity in experimental models (27). In fibrosis field, IFN γ has been well explored as an antifibrotic cytokine due to its direct effects on fibroblasts, and examined in clinical studies for idiopathic pulmonary fibrosis and liver fibrosis, though remained ineffective (13, 14). Main reasons for its clinical failure are its poor pharmacokinetics and severe side effects. IFN γ R is highly expressed on immune cells (28) and numerous other cells in different organs, as shown in Supplementary Fig. S1, which leads to severe systemic adverse effects. Therefore, targeted delivery of IFN γ to specific key disease-inducing cells is prerequisite to enhance its therapeutic efficacy and to reduce its side effects.

Many attempts have been made to deliver IFN γ to tumors using liposomes, polymer gels, microspheres and nanoparticles (32–34). In these approaches, however, cell-selective targeting is lacking which might result in

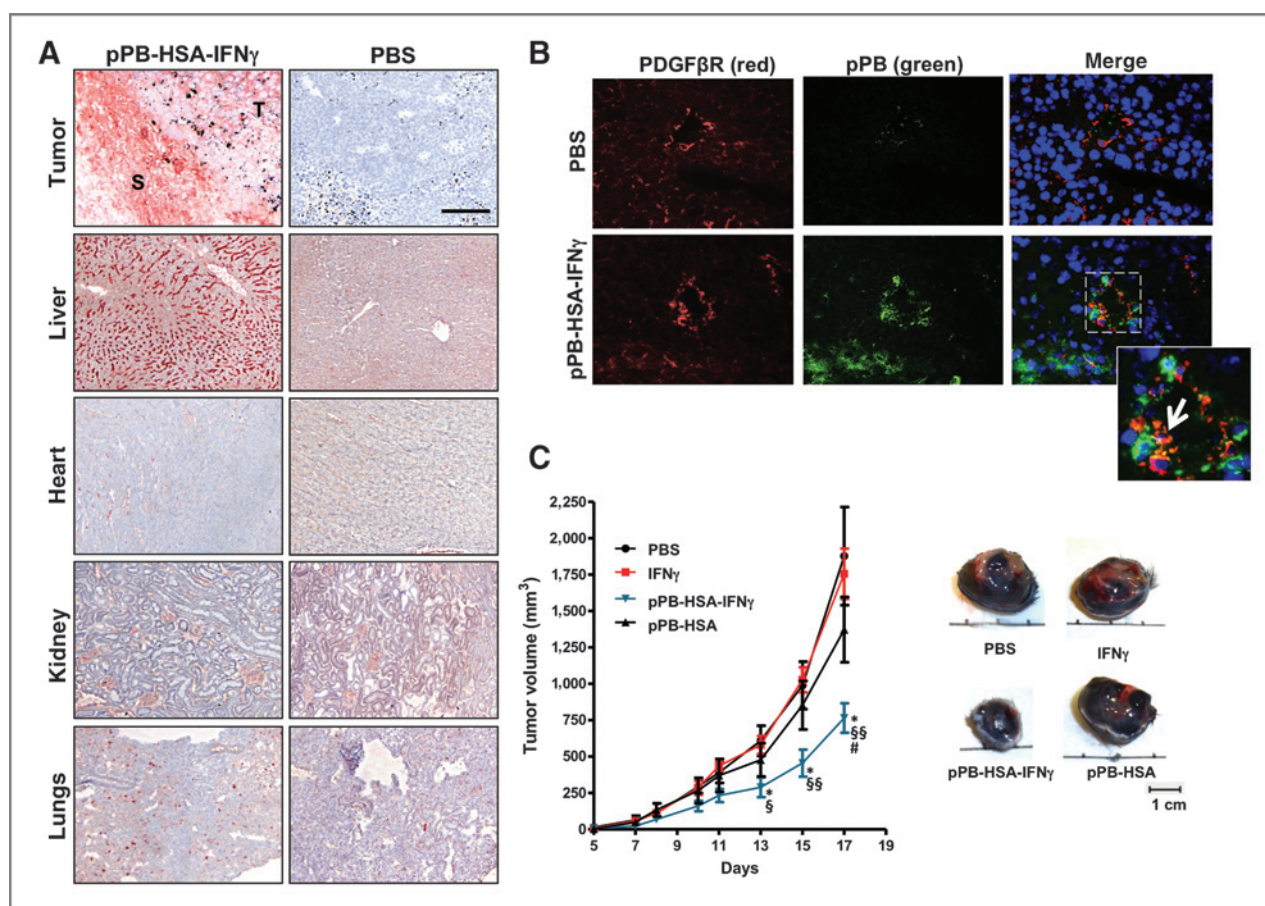


Figure 4. *In vivo* distribution and the therapeutic effects of pPB-HSA-IFN γ in subcutaneous B16 tumor. **A**, the anti-pPB immunostaining illustrates the distribution of the conjugate in tumors and different organs 15 minutes after the intravenous administration of pPB-HSA-IFN γ in B16-tumor bearing mice. Scale bar, 200 μ m. **B**, representative immunofluorescent photographs depicting specific accumulation of pPB-HSA-IFN γ in pericytes. Anti-pPB (green), anti-PDGFR (red), and nuclei counterstained with 4', 6-diamidino-2-phenylindole (blue). Magnification, $\times 400$. **C**, tumor growth curve of B16 tumors following intravenous treatment with PBS ($n = 5$), IFN γ ($n = 5$), pPB-HSA-IFN γ ($n = 5$), and pPB-HSA ($n = 4$). *, $P < 0.05$ versus PBS; §, $P < 0.05$ and §§, $P < 0.01$ versus IFN γ ; #, $P < 0.05$ versus pPB-HSA; unpaired Student t test. Representative pictures of the isolated tumors at the end of the experiment.

systemic side effects in long-term treatment. Delivery of IFN γ specifically to tumor blood vessels using a GCNGRC peptide (NGR) has also been attempted to induce immune-mediated antitumor effects (27). However, IFN γ -NGR construct induced potent antitumor effects at very low doses (0.005 μ g/kg), whereas nontargeted IFN γ induced little or no effect at the dose of 0.003 to 250 μ g/kg. At higher doses, both untargeted and targeted IFN γ were ineffective because of induction of immune-mediated counter-regulatory mechanisms (27), and moreover, multiple treatments at low doses induced resistance to the therapy (35). In the present study, however, we applied a different approach and targeted IFN γ to both stromal fibroblasts and pericytes using a PDGFR-targeting peptide. This strategy has many advantages over other approaches because (i) stromal fibroblasts and pericytes compose the largest component in a tumor providing a large area for targeting; (ii) these cells strongly participate in many tumor-promoting processes, inhibition of which may lead to hampering of tumor growth; (iii) PDGFR

expression is highly expressed on these stromal cells compared with tumor cells and normal tissues; (iv) stromal cells are likely to be more genetically stable and commonly present in multiple tumor types; (v) furthermore, the antitumor effects are mostly exhibited through its antifibrotic activity than immunomodulatory effects, and therefore chances of counter-regulatory mechanisms, as exemplified above, would be minimal.

Both CAFs and pericytes are mesenchymal cell types and commonly express PDGFR and α -SMA whereas pericytes present in normal tissues do not express α -SMA (2, 4). TGF β -activated 3T3 fibroblasts, as shown in this study, had also high expression of these markers, depicting the characteristics of stromal fibroblasts. Inhibition of activation and migration of these cells as well as decrease in the production of extracellular matrix by IFN γ and pPB-HSA-IFN γ indicates the potent antifibrotic effects of these compounds. As expected, free and targeted IFN γ showed similar effects *in vitro* because of no constraints for binding to IFN γ R. The real impact of stromal cells in a tumor is

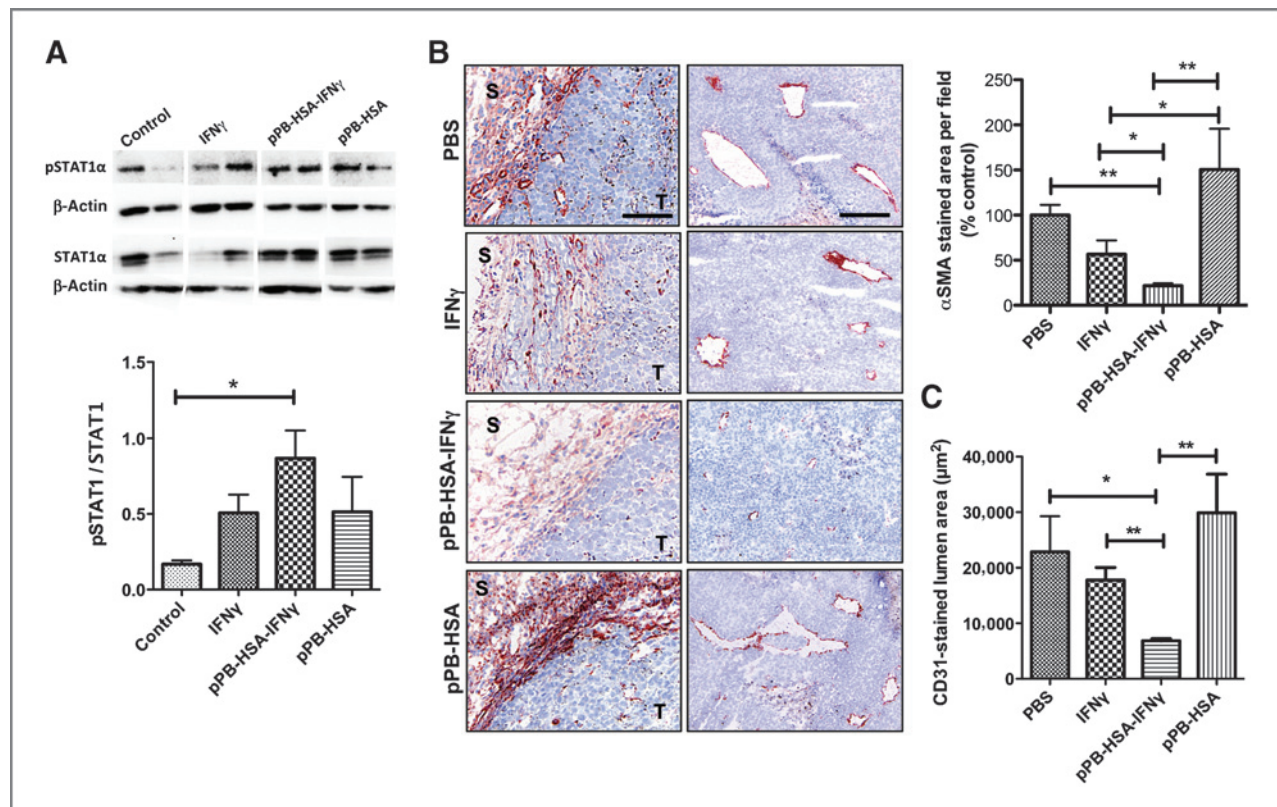


Figure 5. *In vivo* effect of pPB-HSA-IFN γ on stromal fibroblasts and pericytes in subcutaneous B16 tumor-bearing mice. **A**, Western blot analyses of pSTAT-1 α in tumors for pSTAT-1 α and STAT1 α . The pSTAT1 α and STAT1 α bands were quantified and normalized by their respective β -actin controls and then the ratio of pSTAT1 α and STAT1 α was calculated. All the electrophoresed samples were blotted at the same time and blots were analyzed with the same exposure time. $N = 4-5$ mice per group; *, $P < 0.05$. **B**, representative pictures showing immunostaining for α SMA, a marker for fibroblasts and pericytes, in stromal fibrous capsule (S), tumor (T), and around blood vessels. Scale bar, 200 μ m. Quantitative analyses of α SMA immunostaining in tumors using image analysis software. **C**, bar graph showing the lumen area of tumor blood vessels analyzed after CD31 immunostaining on tumor sections. Unpaired Student *t* test; *, $P < 0.05$; **, $P < 0.01$.

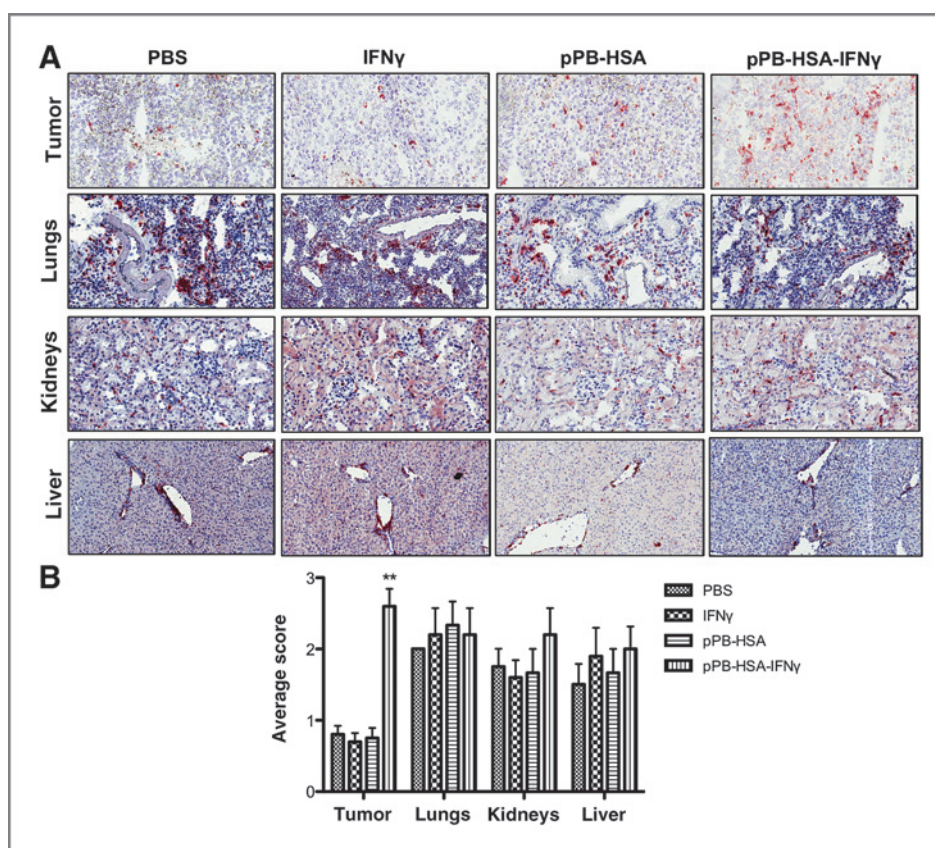
exerted by their strong paracrine actions through which they induce angiogenesis, invasion, metastasis, and tumorigenesis (2, 4). Through the paracrine mimicking *in vitro* experiments, we showed that treatment of fibroblasts with targeted IFN γ strongly inhibited the fibroblasts-induced tube formation of endothelial cells. These data support the notion that the selective inhibition of stromal cells *in vivo* may inhibit their paracrine action and thereby the tumor growth.

Cell-selective targeting *in vivo* is a challenging task mainly due to nonspecificity of a target receptor. In our approach, targeting to stromal cells through PDGF β R caused a rapid accumulation of pPB-HSA-IFN γ in tumor stroma and pericytes in subcutaneous tumors. Although PDGF β R is known to be expressed on many cell types in different organs, as a matter of fact its expression is mainly high during early developmental stages but quite low in normal tissues (36, 37). In many pathologic conditions, PDGF β R expression increases remarkably, especially in fibrotic diseases and in tumor stroma (2, 38). For the same reason, we found a negligible distribution of pPB-HSA-IFN γ in normal organs

except in liver sinusoids, which is most likely due to its presence in circulation. We have shown in an earlier study that a pPB-HSA-doxorubicin conjugate was visible in liver sinusoids after 30 minutes of an intravenous injection but disappeared after 2 hours (22). Moreover, in the present study no significant induction in MHC-II and CD68 expression in livers with the conjugate clearly indicates no side effect in liver. These data further signifies the tumor specificity of the therapy.

The potential benefits of the targeted approach were observed *in vivo* where targeted IFN γ significantly reduced the tumor growth while untargeted IFN γ (at the equivalent dose) was ineffective. A substantial induction of pSTAT1 α expression in tumors by pPB-HSA-IFN γ confirmed its IFN γ -mediated local effects. In contrast, free IFN γ or the carrier did not significantly enhance the pSTAT1 α in tumors. Reduction in α SMA expression in the tumor-associated fibrous tissue and around blood vessels with targeted IFN γ clearly showed the deactivation and/or reduction of fibroblasts and pericytes, which resulted in the antitumor effects. In addition, no increase in tumor macrophage or lymphocytes infiltration in the

Figure 6. *In vivo* expression of MHC-II in tumors and different organs in B16 tumor-bearing mice. **A**, representative microscopic pictures of MHC-II staining in tumors and different organs. Magnification, $\times 200$, except livers ($\times 100$). **B**, semiquantitative analyses of MHC-II staining showing the average score (\pm SEM) in tumors and other organs. $n = 4$ –5 mice/group for tumors and $n \geq 3$ mice/group for other organs. Unpaired Student *t* test; **, $P < 0.01$ versus PBS, IFN γ , and pPB-HSA groups. The whole section was scored using the following scoring criteria. Negative section (score 0.5), occasionally positive cells (score 1), a significant number of positive cells with some negative area (score 2), and areas with strong positive cells but still negative areas (score 3). No tumor or any other organ was completely positive.



conjugate-treated animals further supports the direct effect on the targeted cells. As pericytes are directly involved in blood vessel maturation, contribution of pericyte inhibition for antitumor effects is more evident than that of fibroblast inhibition. However, it is difficult to delineate the role of different cell types for these effects.

Induction of systemic side effects by IFN γ has been a major reason for the failure in clinical trials (11). However, at the used doses we did not see any side effect of free IFN γ on body weight and hematologic parameters. Also in MHC-II staining analysis, untargeted IFN γ did not induce its expression in tumors and other organs while the conjugate induced it only in tumors (see Fig. 6). As IFN γ itself did not show side effects at the injected doses, no further improvements were expected from targeted IFN γ .

In conclusion, this study reveals a novel approach to deliver IFN γ to stromal fibroblasts and pericytes using our PDGFR β -targeting carrier. Blockade of the activation of these cells by targeted IFN γ construct leads to a reduction in tumor growth. These data may form a strong base to develop a novel therapeutic compound for the treatment of cancer as well as provide new opportunities to use cytokines as therapeutic compounds.

Disclosure of Potential Conflicts of Interest

K. Poelstra is a co-inventor of pPB-HSA patent and is a co-founder and CSO of Biorion Technologies, Netherlands and holds <5% stocks in the company. J. Prakash is VP Preclinical, Biorion Technologies and acts as an

advisory member. No potential conflicts of interest were disclosed for other authors.

Authors' Contributions

Conception and design: R. Bansal, K. Poelstra, J. Prakash
Development of methodology: R. Bansal, T. Tomar, J. Prakash
Acquisition of data (provided animals, acquired and managed patients, provided facilities, etc.): R. Bansal, T. Tomar, J. Prakash
Analysis and interpretation of data (e.g., statistical analysis, biostatistics, computational analysis): R. Bansal, T. Tomar, A. Ostman, K. Poelstra, J. Prakash
Writing, review, and/or revision of the manuscript: R. Bansal, A. Ostman, K. Poelstra, J. Prakash
Administrative, technical, or material support (i.e., reporting or organizing data, constructing databases): J. Prakash
Study supervision: K. Poelstra, J. Prakash

Acknowledgments

Authors thank Eduard Post and Catharina Reker-Smit for their technical support; and Leonie Beljaars and Marlies Schippers for their help in immunohistochemical staining.

Grant Support

K. Poelstra received a European Union sponsored Innovative Action Program Groningen (IAG2) Netherlands and VICI grant from the Dutch Technology Foundation (STW) and Organization for Scientific Research (NWO), The Netherlands. J. Prakash received a Swedish Cancer Foundation Postdoctoral grant and a European Union Marie Curie Career Integration grant (#283973).

The costs of publication of this article were defrayed in part by the payment of page charges. This article must therefore be hereby marked *advertisement* in accordance with 18 U.S.C. Section 1734 solely to indicate this fact.

Received September 20, 2011; revised August 8, 2012; accepted August 23, 2012; published OnlineFirst August 29, 2012.

References

- Hanahan D, Weinberg RA. Hallmarks of cancer: the next generation. *Cell* 2011;144:646–74.
- Pietras K, Ostman A. Hallmarks of cancer: interactions with the tumor stroma. *Exp Cell Res* 2010;316:1324–31.
- Kalluri R, Zeisberg M. Fibroblasts in cancer. *Nat Rev Cancer* 2006;6:392–401.
- Ostman A, Augsten M. Cancer-associated fibroblasts and tumor growth—bystanders turning into key players. *Curr Opin Genet Dev* 2009;19:67–73.
- Paulsson J, Sjoblom T, Micke P, Ponten F, Landberg G, Heldin CH, et al. Prognostic significance of stromal platelet-derived growth factor beta-receptor expression in human breast cancer. *Am J Pathol* 2009;175:334–41.
- Hagglof C, Hammarsten P, Josefsson A, Stattin P, Paulsson J, Bergh A, et al. Stromal PDGFRbeta expression in prostate tumors and non-malignant prostate tissue predicts prostate cancer survival. *PLoS One* 2010;5:e10747.
- Pietras K, Stumm M, Hubert M, Buchdunger E, Rubin K, Heldin CH, et al. STI571 enhances the therapeutic index of epothilone B by a tumor-selective increase of drug uptake. *Clin Cancer Res* 2003;9:3779–87.
- Pietras K, Hanahan D. A multitargeted, metronomic, and maximum-tolerated dose "chemo-switch" regimen is antiangiogenic, producing objective responses and survival benefit in a mouse model of cancer. *J Clin Oncol* 2005;23:939–52.
- De ME, De Maeyer-Guignard J. Interferon-gamma. *Curr Opin Immunol* 1992;4:321–6.
- Borden EC, Sen GC, Uze G, Silverman RH, Ransohoff RM, Foster GR, et al. Interferons at age 50: past, current and future impact on biomedicine. *Nat Rev Drug Discov* 2007;6:975–90.
- Miller CH, Maher SG, Young HA. Clinical use of interferon-gamma. *Ann N Y Acad Sci* 2009;1182:69–79.
- Ikeda H, Old LJ, Schreiber RD. The roles of IFN gamma in protection against tumor development and cancer immunoediting. *Cytokine Growth Factor Rev* 2002;13:95–109.
- King TE Jr, Albera C, Bradford WZ, Costabel U, Hormel P, Lancaster L, et al. Effect of interferon gamma-1b on survival in patients with idiopathic pulmonary fibrosis (INSPIRE): a multicentre, randomised, placebo-controlled trial. *Lancet* 2009;374:222–8.
- Pockros PJ, Jeffers L, Afdhal N, Goodman ZD, Nelson D, Gish RG, et al. Final results of a double-blind, placebo-controlled trial of the antifibrotic efficacy of interferon-gamma1b in chronic hepatitis C patients with advanced fibrosis or cirrhosis. *Hepatology* 2007;45:569–78.
- Gleave ME, Elhilali M, Fradet Y, Davis I, Venner P, Saad F, et al. Interferon gamma-1b compared with placebo in metastatic renal-cell carcinoma. Canadian Urologic Oncology Group. *N Engl J Med* 1998;338:1265–71.
- Schiller JH, Pugh M, Kirkwood JM, Karp D, Larson M, Borden E. Eastern cooperative group trial of interferon gamma in metastatic melanoma: an innovative study design. *Clin Cancer Res* 1996;2:29–36.
- Baroni GS, D'Ambrosio L, Curto P, Casini A, Mancini R, Jezequel AM, et al. Interferon gamma decreases hepatic stellate cell activation and extracellular matrix deposition in rat liver fibrosis. *Hepatology* 1996;23:1189–99.
- Oldroyd SD, Thomas GL, Gabbiani G, El Nahas AM. Interferon-gamma inhibits experimental renal fibrosis. *Kidney Int* 1999;56:2116–27.
- Rockey DC, Chung JJ. Interferon gamma inhibits lipocyte activation and extracellular matrix mRNA expression during experimental liver injury: implications for treatment of hepatic fibrosis. *J Invest Med* 1994;42:660–70.
- Ziesche R, Hofbauer E, Wittmann K, Petkov V, Block LH. A preliminary study of long-term treatment with interferon gamma-1b and low-dose prednisolone in patients with idiopathic pulmonary fibrosis. *N Engl J Med* 1999;341:1264–9.
- Beljaars L, Weert B, Geerts A, Meijer DK, Poelstra K. The preferential homing of a platelet derived growth factor receptor-recognizing macromolecule to fibroblast-like cells in fibrotic tissue. *Biochem Pharmacol* 2003;66:1307–17.
- Prakash J, de JE, Post E, Gouw AS, Beljaars L, Poelstra K. A novel approach to deliver anticancer drugs to key cell types in tumors using a PDGF receptor-binding cyclic peptide containing carrier. *J Control Release* 2010;145:91–101.
- Bansal R, Prakash J, Post E, Beljaars L, Schuppan D, Poelstra K. Novel engineered targeted interferon-gamma blocks hepatic fibrogenesis in mice. *Hepatology* 2011;54:586–96.
- Bansal R, Prakash J, de Ruijter M, Beljaars L, Poelstra K. Peptide modified-albumin carrier explored as a novel strategy for a cell-specific delivery of interferon gamma to treat liver fibrosis. *Mol Pharm* 2011;8:1899–909.
- Wang JH, Wu QD, Bouchier-Hayes D, Redmond HP. Hypoxia upregulates Bcl-2 expression and suppresses interferon-gamma induced antiangiogenic activity in human tumor derived endothelial cells. *Cancer* 2002;94:2745–55.
- Bansal R, Post E, Proost JH, de Jager-Krikken A, Poelstra K, Prakash J. PEGylation improves pharmacokinetic profile, liver uptake and efficacy of Interferon gamma in liver fibrosis. *J Control Release* 2011;154:233–40.
- Curnis F, Gasparri A, Sacchi A, Cattaneo A, Magni F, Corti A. Targeted delivery of IFNgamma to tumor vessels uncouples antitumor from counterregulatory mechanisms. *Cancer Res* 2005;65:2906–13.
- Schroder K, Hertzog PJ, Ravasi T, Hume DA. Interferon-gamma: an overview of signals, mechanisms and functions. *J Leukoc Biol* 2004;75:163–89.
- Santos AM, Jung J, Aziz N, Kissil JL, Pure E. Targeting fibroblast activation protein inhibits tumor stromagenesis and growth in mice. *J Clin Invest* 2009;119:3613–25.
- Sumida T, Kitadai Y, Shinagawa K, Tanaka M, Kodama M, Ohnishi M, et al. Anti-stromal therapy with imatinib inhibits growth and metastasis of gastric carcinoma in an orthotopic nude mouse model. *Int J Cancer* 2011;128:2050–62.
- Olive KP, Jacobetz MA, Davidson CJ, Gopinathan A, McIntyre D, Honess D, et al. Inhibition of Hedgehog signaling enhances delivery of chemotherapy in a mouse model of pancreatic cancer. *Science* 2009;324:1457–61.
- Mejias R, Perez-Yague S, Gutierrez L, Cabrera LI, Spada R, Acedo P, et al. Dimercaptosuccinic acid-coated magnetite nanoparticles for magnetically guided *in vivo* delivery of interferon gamma for cancer immunotherapy. *Biomaterials* 2011;32:2938–52.
- van Slooten ML, Storm G, Zoepfel A, Kupcu Z, Boerman O, Crommelin DJ, et al. Liposomes containing interferon-gamma as adjuvant in tumor cell vaccines. *Pharm Res* 2000;17:42–8.
- Younes HM, Amsden BG. Interferon-gamma therapy: evaluation of routes of administration and delivery systems. *J Pharm Sci* 2002;91:2–17.
- Gasparri AM, Jachetti E, Colombo B, Sacchi A, Curnis F, Rizzardi GP, et al. Critical role of indoleamine 2,3-dioxygenase in tumor resistance to repeated treatments with targeted IFNgamma. *Mol Cancer Ther* 2008;7:3859–66.
- Alvarez RH, Kantarjian HM, Cortes JE. Biology of platelet-derived growth factor and its involvement in disease. *Mayo Clin Proc* 2006;81:1241–57.
- Andrae J, Gallini R, Betsholtz C. Role of platelet-derived growth factors in physiology and medicine. *Genes Dev* 2008;22:1276–312.
- Barrett TB, Seifert RA, Bowen-Pope DF. Regulation of platelet-derived growth factor receptor expression by cell context overrides regulation by cytokines. *J Cell Physiol* 1996;169:126–38.